



International Journal of
Cancer Research

ISSN 1811-9727



Academic
Journals Inc.

www.academicjournals.com



Research Article

Analysis of Sensitivity and Cell Death Pathways Mediated by Anti-cancer Drugs Using Three-dimensional Culture System

¹Takeshi Kinoshita, ^{1,2}Hajime Higuchi, ^{1,3}Ayano-Kabashima-Niibe, ^{1,4}Gen Sakai, ^{1,5}Yasuo Hamamoto, ^{1,5}Hiromasa Takaishi and ¹Takanori Kanai

¹Department of Internal Medicine, Keio University School of Medicine, 35 Shinanomachi, Shinjyuku-ku, 160-8582 Tokyo, Japan

²Digestive Disease Center, International University of Health and Welfare, 1-4-3 Mita, Minato-ku, 108-8329 Tokyo, Japan

³Center for Basic Research in Digestive Diseases, Mayo Clinic, 200 First Street South West, Rochester, 55905 MN, Minnesota, USA

⁴Department of Internal Medicine, Tokyo Saiseikai Central Hospital, 1-4-17 Mita, Minato-ku, 108-0073 Tokyo, Japan

⁵Keio Cancer Center, Keio University School of Medicine, 35 Shinanomachi, Shinjyuku-ku, 160-8582 Tokyo, Japan

Abstract

Objective: The aim of this study was to evaluate the differences of cytotoxicity mediated by anti-cancer drugs between 2D and 3D culture conditions. **Methodology:** The colon cancer cell line HCT116 was cultured in 2D and 3D conditions. Anti-proliferation effects and cell death pathways of cytotoxic agents, i.e., SN-38 and multi-kinase inhibitors i.e., sorafenib were examined. Data was analyzed by Student's t-test. **Results:** Although SN-38 induced significant apoptosis associated with caspase-3/7 activation in 2D condition, apoptosis and anti-proliferation effects of SN-38 dramatically diminished in 3D condition. In contrast, anti-proliferation effects mediated by sorafenib unchanged. Interestingly, sorafenib induced significant apoptosis in the cells locating in the center of the 3D spheroids, whereas it did not induce caspase activation in 2D condition. In addition, 2D culture with low glucose concentration, a model mimicking central condition of the spheroids, revealed the significant cell death with caspase activation by sorafenib. **Conclusion:** 3D culture system provide new findings regarding cytotoxicity of compounds which are not identified by the 2D culture.

Key words: Apoptosis, drug-sensitivity, autophagy, 2D vs 3D, cell death conversion

Citation: Takeshi Kinoshita, Hajime Higuchi, Ayano-Kabashima-Niibe, Gen Sakai, Yasuo Hamamoto, Hiromasa Takaishi and Takanori Kanai, 2018. Analysis of sensitivity and cell death pathways mediated by anti-cancer drugs using three-dimensional culture system. *Int. J. Cancer Res.*, 14: 1-12.

Corresponding Author: Hajime Higuchi, Digestive Disease Center, International University of Health and Welfare, 1-4-3 Mita, Minato-ku, 108-8329 Tokyo, Japan Tel: +81-3-3451-8121 (ext. 5560) Fax: +81-3-3454-0067

Copyright: © 2018 Takeshi Kinoshita *et al.* This is an open access article distributed under the terms of the creative commons attribution License, which permits unrestricted use, distribution and reproduction in any medium, provided the original author and source are credited.

Competing Interest: The authors have declared that no competing interest exists.

Data Availability: All relevant data are within the paper and its supporting information files.

INTRODUCTION

Although *in vitro* cell culture system is handy and expected as initial anti-cancer drug screening tests for the sensitivity of cancer cells, the most of potential anti-cancer drugs come from the cell culture system-based approaches failed during clinical trials because of low efficacy or unexpected toxicity^{1,2}. One reason for the very low efficiency is that the most drug screening tests may rely on the *in vitro* drug sensitivity tests using 2D culture system. It has been suggested that 2D culture system has limitations, i.e., 2D cultured cells lack of cell-cell and cell-extracellular matrix (ECM) signaling^{3,4}. Hence, 3D culture system was expected as one of the methods to solve these problems. In this culture system, cells show many phenotypes heterogeneously including cell-cell or cell-ECM interactions that also occur *in vivo*^{5,6}. Thus, 3D culture system is thought as a potential link to bridge the gap between *in vitro* and *in vivo*.

In this past decade, many molecular target drugs have been developed. They have shown clear clinical benefits in response rate, progress free survival and even overall survival. Currently, multi-kinase inhibitors whose target molecules are tyrosine-kinase associated with relatively broad range of cell surface receptors, i.e., VEGFR, PDGFR, KIT, RET, etc. Sorafenib was proposed as effective multi-kinase inhibitor against advanced refractory solid tumors including metastatic colorectal cancer (mCRC) in the early phase I study⁷ and demonstrated the overall clinical benefits against advanced clear cell renal cell carcinoma and advanced thyroid tumor^{8,9}. Recently, pazopanib was approved for first-line therapy of advanced renal cell carcinoma^{10,11} and regorafenib, an analog of sorafenib, showed the survival benefits in the phase III studies¹²⁻¹⁴.

Sorafenib is one of the early developed multi-kinase inhibitors, currently represents the primary treatment option for advanced solid tumors including hepatocellular carcinoma^{15,16}. Recently, sorafenib has been combined with multiple cytotoxic therapies in the clinic trials including cetuximab for mCRC¹⁷. Sorafenib targets in particular the B-raf kinase activity and VEGFR tyrosine kinase activity. However, it was also reported that sorafenib has the effect on cellular metabolism that is independent of the kinase inhibitory activity and that contributes to anti-cancer effect of this compound^{18,19}. Thus, precise mechanisms by which sorafenib exerts the anti-cancer activity are not fully understood.

In the present study, 3D spheroid culture using commercially available NanoCulture plate (NCP) was used to compare the anti-cancer cell effects between conventional chemotherapeutic drugs and selected multi-kinase inhibitors.

As a result, cancer cell death induced by cytotoxic chemotherapeutic agents with different sensitivity under 2D or 3D culture conditions were identified. In addition, multi-kinase inhibitors mediated cancer cell death in both 2D and 3D conditions, while distinct types of cell death, i.e., apoptotic cell death or non-apoptotic cell death were induced according to the culture condition. These results provide new insights regarding the mechanisms by which multi-kinase inhibitors induce cancer cell death. Thus, 3D culture using the NCP would be an attractive technology to evaluate anti-cancer cell activities of the drugs readily, partly mimicking *in vivo* conditions.

MATERIALS AND METHODS

Cell line and cell culture: The human colon cell line HCT116 were cultured in RPMI1640 medium supplemented with 10% heat-inactivated fetal bovine serum (FBS), 50 $\mu\text{g mL}^{-1}$ streptomycin and 60 $\mu\text{g mL}^{-1}$ penicillin. The cell line was kept at 37°C in a humidified incubator containing 5% CO₂. The cell line was split one eighth in a week and morphology and growth of cells were monitored on a weekly basis. Hypoxic culture was done by using incubator containing 0.2% O₂.

3D culture of spheroids: The cell line pre-cultured in conventional condition was harvested and seeded into 24 or 96 well NanoCulture plate (SCIVAX, Kanagawa Japan) at the density of 1×10^4 cells mL⁻¹. The plates were incubated at 37°C in 5% CO₂ for a week and cells formed spheroids. Morphology and growth of cell were monitored. For test the effects of compounds against related cells, 7 day cultured spheroids were harvested into eppendorf tube and centrifuged (3,000 rpm, 3 min) followed by washing once with PBS. Then, spheroids were treated with Trypsin/EDTA (Thermo Fisher Scientific, 25300054) for 5 min and washed once with culture medium. Single cells were collected by using cell strainer and seeded into normal plate at the density of 1×10^4 cells mL⁻¹.

Morphology and immunohistochemistry (IHC): Three and 7 day old spheroids cultured in NCP were harvested into eppendorf tube and centrifuged (room temperature, 3,000 rpm, 3 min). Then spheroids were washed once with PBS and embedded into collagen gels. Embedded spheroids were fixed by adding paraformaldehyde (room temperature, 10 min) followed by washing three times with PBS and collagen gels including fixed spheroids were embedded in paraffin followed by sectioning according to standard protocol.

Gene expression analysis: Total RNA was isolated using RNeasy Mini Kit (Qiagen, Hilden, Germany, 74104) and immediately stored at -20°C until further use. RNA purity was measured by using ND1000 spectrophotometer (NanoDrop technologies, Wilmington, DE, USA). Starting from 5 µg of total RNA, cDNA synthesis was performed using PrimeScript kit (TAKARA, Shiga, Japan, 2690A) according to the technical manual. Then, quantitative reverse transcription polymerase chain reaction assays (q-RT-PCR) was performed using StepOnePlus Real-time PCR System (Applied Biosystems Life Technologies Japan) with Fast Universal Master Mix according to manufacturer's instructions. The variation in the initial amount of total RNA in the different samples was normalized in every assay using GAPDH gene expression as an internal standard.

Cell cycle analysis: Cell cycle analysis was performed by using BrdU Flow Kit (BD Pharmingen Japan, 559619). Briefly, new DNA synthesis was measured by detecting incorporated nucleoside analogs and total DNA content were measured using DNA dyes 7-AAD.

Measurement of cell viability: In 2D proliferation assay, 100 µL cell suspension with 1×10^3 cells were seeded into each well on day 1 of experiment. On day 2, compound solutions were diluted in medium at three times the desired final concentration and 50 µL of that were added to each well. In 3D proliferation assay, 50 µL of compound solution prepared as described above were added to 7 day old spheroids. In each assay, compounds exposed cells were incubated in CO₂ incubator for 72 h at 37°C in 5% CO₂ before assessment of cell viability and duplicate wells were used for each drug and concentration in all experiment. Twelve wells added DMSO containing medium were served as control and twelve wells containing only culture medium were served as blank. Cell viability was estimated by measuring cellular ATP contents (TOYO INK, Japan, CA50). Fifty µL of reagent were added to each well and the plates were incubated at 37°C for 10 min after shaking. Then luminescence was measured using plate reader (Tecan, M1000PRO). Cell viability was calculated as the mean luminescence of drug exposed wells in percent of that of control wells with luminescence of blank wells subtracted.

Caspase activity assay: Caspase-3/7 activity was measured by using Caspase-Glo 3/7 assay (Promega, Madison, WI, USA, G8091). 100 µL of Caspase-Glo 3/7 reagent was added to the each well and incubated for 30 min at 37, then luminescence was measured by plate reader. Caspase activity was calculated

as the mean luminescence of drug exposed wells in percent of that of control wells with luminescence of blank wells subtracted.

Western blot: HCT116 cells cultured in 6 well conventional plate or 24 well NCP were harvested and lysed in lysis buffer (Cell signaling technology (CST), Beverly, MA, USA, 9803s) and stored at -20°C until further analysis. Cell lysates were subjected to SDS-PAGE on a 5-10% polyacrylamide gel. Then, proteins were electroblotted onto a PVDF membrane (Millipore Corp., Bedford, MA, USA). After blocking with Blocking One reagent (Nacalai, 03953-95), membranes were treated with the primary antibody. Primary antibodies were diluted in Blocking One reagent at the following dilutions: Anti-cleaved caspase-3 antibodies (1:1000), anti-LC3B antibodies (1:1000) and anti-b-actin (1:10000), incubated overnight at 4°C. Subsequently, membranes were washed 3 times with TBS in Tween-20 and counterstained with the corresponding secondary antibodies conjugated to anti-rabbit (CST, 7076S) or anti-mouse IgG (CST, 7074S) (1:5000). The membranes were visualized using pierce enhanced chemiluminescence (ECL) Western blotting reagents and ECL film.

Drugs and antibodies: The conventional cytotoxic compounds, i.e., paclitaxel, gemcitabine, trichostatin A and SN-38 were from Sigma-Aldrich (St. Louis, MO, USA). The molecular target agents, i.e., gefitinib were from Sigma-Aldrich, AG17, regorafenib and sorafenib were from Funakoshi (Tokyo, Japan). Primary antibodies against Ki-67 (Dako, Japan, M7240), LC3B (CST, Beverly, MA, USA, 3868T), cleaved-caspase-3 (CST. 9664T) and b-actin (Santa cruz, Danvers, MA, USA, sc-47778) were used to assess the expression of these molecules.

Statistical analysis: Statistical analysis was performed by Student's t-test. $p < 0.05$ was considered statistically significant.

RESULTS

Characteristics of HCT116 spheroids formed in NCP: HCT116 cells cultured on NCP started to aggregate on the first day after seeding. The surface of HCT116 aggregates were enclosed by a membrane-like structure, forming a spheroid-like structure on day 3. The HCT116 spheroids grew larger, reaching diameter at $160 \mu\text{m} \pm 25 \mu\text{m}$ on day 7 (Fig. 1a).

To confirm the proliferation status of the spheroids, cell cycle was analyzed by BrdU incorporation assay using flow

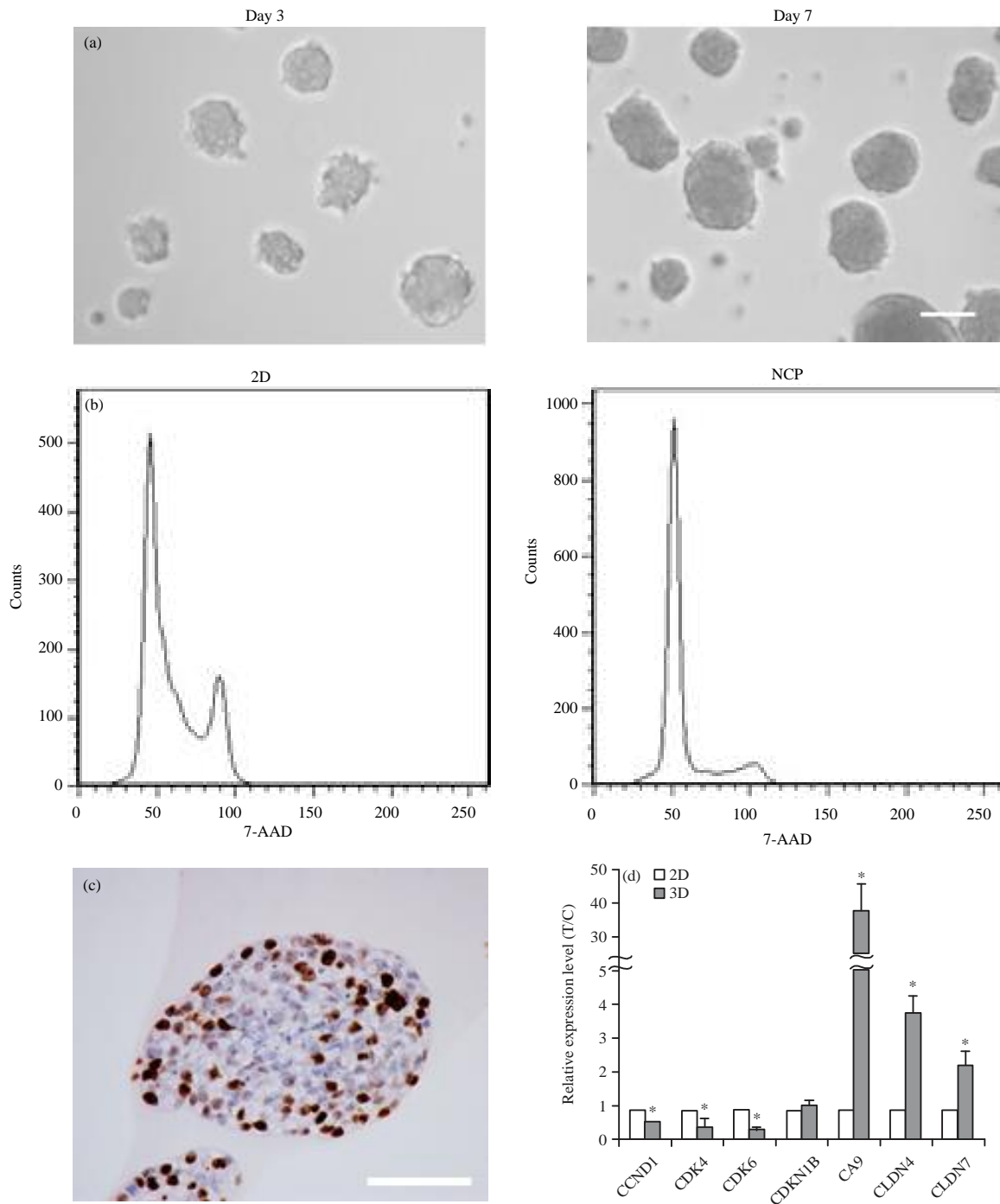


Fig. 1(a-d): Colorectal cell line HCT116 cultured in NCP showed typical phenotypes observed in 3D culture condition (a) Microscope images of HCT116 cells cultured for 3 days (left panel) and 7 days (right panel) in NCP. Scale bar indicated 100 μ m, (b) Cell cycle analysis of HCT116 cells cultured in conventional plate for 24 h (left panel) and cultured in NCP for 7 days, (c) Immunohistochemical analysis of Ki-67 in HCT116 cells cultured in NCP for 7 days. Scale bar indicated 100 μ m and (d) Gene expression analysis of HCT116 spheroids cultured for 7 days in NCP. Data was expressed as the ratio of target mRNA to GAPDH mRNA

Experiment was conducted three times, each sample was assessed in duplicate. Each bar represents the Mean \pm SD. (n = 3), *p<0.05 compared with 2D culture group

cytometry (Fig. 1b). On day 7 of the 3D culture, the percentage of cells in G0/G1 phase was 79.2%, while the percentage of G0/G1 phase was 38.4% in the cells cultured with 2D system. The percentage of cells in G2/S phase decreased by the 3D culture as compared with the 2D culture (4.7 and 10.8%, respectively). These results suggest that the majority of the cells within 7 day old 3D spheroids were not in proliferative phase. Next, Ki-67 expression was evaluated by immuno-staining. In 7 day old spheroids, only cells located periphery of the spheroids expressed Ki-67, while the cells located in the central area did not express Ki-67 (Fig.1c).

Gene expression was analyzed to investigate if there is any change in 2D and 3D conditions. Expression of genes associated with cell growth and DNA replication, i.e., CCND1, CCND3, CCNE2, CDK4 and CDK6 were strongly suppressed and expression of CDKN1B which negatively regulates these cyclins and CDKs was not altered (Fig.1d). On the other hands, carbonic anhydrase 9 (CA9, a target gene of HIF1a) and tight junction marker, i.e., claudin-4 (CLDN4) and claudin-7 (CLDN7) were markedly up-regulated in the spheroids.

Drug sensitivity: To examine the drug sensitivities against conventional cytotoxic compounds and molecular target compounds, antiproliferative assay was performed in 2D and 3D conditions as described in the material and method. Although conventional cytotoxic compounds, i.e., paclitaxel, gemcitabine, trichostatin A and SN-38, strongly inhibited proliferation of HCT116 cells in 2D culture condition, the growth inhibitory effects of these compounds dramatically decreased in 3D culture condition (Fig.2a). For example, the IC₅₀ value of paclitaxel was less than 0.1 μM in the 2D culture condition, nevertheless 3D spheroid cells were relatively resistant to paclitaxel with IC₅₀ value over 10μM. In contrast to conventional compounds, the growth inhibitory effects of molecular target agents, i.e., gefitinib, AG17, regorafenib and sorafenib, were not diminished under 3D spheroid condition (Fig.2a). Based on these results, SN-38 was used as a typical conventional compound and sorafenib as a representative molecular target agent for the following experiments.

For further evaluation of the growth inhibitory effects of SN-38 and sorafenib, antiproliferative assay against the cells which were re-plated onto 2D culture dishes after 7 days culture in 3D condition was performed (Fig. 2b). The resistance to SN-38 growth inhibition by 3D spheroid culture was completely canceled by re-plating to 2D culture condition, suggesting the SN-38 resistance observed in 3D culture was reversible.

Analysis of cell death pathway in 3D culture condition: The cell death pathway induced by either SN-38 or sorafenib was evaluated to investigate the mechanism relate to the differences of compound activity between 2D and 3D conditions. First, caspase activity was assessed using luminescent enzyme activity assay caspase-3-Glo (Fig. 3a). SN-38 strongly induced caspase-3/7 activity in 2D culture condition. However, caspase-3/7 activation in 3D culture condition was limited on the first day of the incubation and delayed activation was observed on day 2. On the other hand, sorafenib induced significant cell death in 2D culture condition without caspase-3/7 activation. Interestingly, the caspase-3/7 activation appeared to be induced by sorafenib in 3D spheroids, though the magnitude of caspase activation was limited as the maximum activation was only 2 fold of the control. Then, caspase-3 activation was analyzed by immunoblotting (Fig. 3b). SN-38 induced active caspase-3 fragments in both 2D and 3D culture conditions. Although sorafenib did not induce caspase-3 fragments in 2D culture condition, it induced delayed caspase-3 fragments in 3D culture condition. These results were consistent with the results of caspase-3-Glo assay and evoked the possibility that caspase-independent cell death pathway may mediate sorafenib induced cell death.

Next, LC3-cleavage, a marker of autophagy associated cell death pathway independent from caspase activity, was evaluated (Fig. 3b). Sorafenib mediated LC3-cleavage was obviously identified in both 2D and 3D culture conditions and the magnitude of the active LC3 bands on the immunoblot appears to be more as compared with the bands induced by SN-38. Interestingly, sorafenib induced both significant LC3 activation and minimal caspase activation in the 3D condition. These results suggest that sorafenib induced cell death is mediated by the distinct mechanisms between the 2D and 3D culture conditions.

Then, immunohistochemistry was performed to analyze the localization of active caspase-3 and LC3B as *in situ* markers of apoptosis and autophagy associated cell death, respectively. As expected, SN-38 induced caspase activation was identified within the spheroids. The cells located in the periphery of the spheroids tended to be stained more by the active caspase-3. The LC3B positive cells were minimally identified after SN-38 treatment, suggesting that autophagy associated cell death mechanisms are not cooperative in the SN-38 mediated cell death. In contrast, in sorafenib treated spheroids, the active casepase 3 positive cells were modestly observed in the periphery of the spheroids and identified

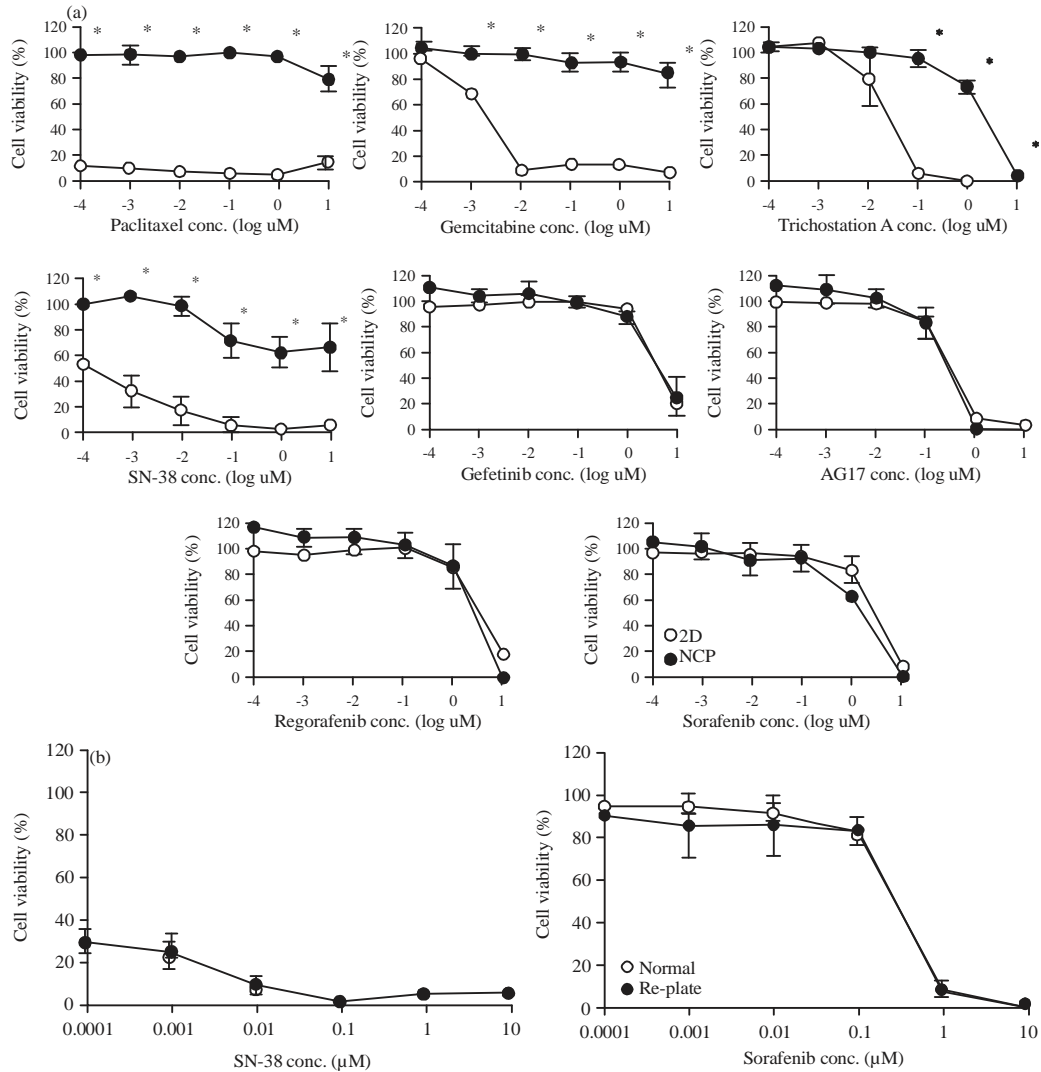


Fig. 2(a-b): Effects of compounds on proliferation in 2D culture and 3D culture condition, (a) Growth inhibitory effects of compounds on proliferation in 2D and 3D culture conditions. HCT116 cells cultured in normal condition and spheroids cultured in NCP were exposed to various compounds for 72 h in various concentration, (b) Effects of SN-38 and sorafenib on proliferation in normal 2D condition and re-plate condition

Experiment was conducted three times, each sample was assessed in duplicate for each drug concentration. Each bar represents the Mean \pm S.D. (n = 3). *p < 0.05 compared with 2D-culture group

rather in the central area (Fig. 3c). More importantly, the LC3B positive cells and the caspase activated cells were mutually exclusive, as LC3B positive cells were located in the periphery of the sorafenib treated spheroids.

Finally, localization of dead cells was identified within the spheroids using plasma membrane impermeable dsDNA binding cell death identifying reagent SYTOX. SYTOX positive cell death was identified strongly in the periphery of the SN-38-treated spheroids and the number of the positive cells gradually decreased toward the central area of the spheroids (Fig. 3d). The localization of the SYTOX positive

cells was similar to the localization of the active caspase-3 positive cells within the SN-38 treated spheroids. In contrast, the SYTOX positive cells were identified mainly in central area of the sorafenib treated spheroids. The localization of dead cells in SN-38 treated spheroids or sorafenib treated spheroids appeared to relate to the localization of caspase-3 activated cells.

Analysis of cell death in low glucose or hypoxic culture condition: The localization of dead cells marked by caspase labeling or SYTOX assay suggests that types of cell death or

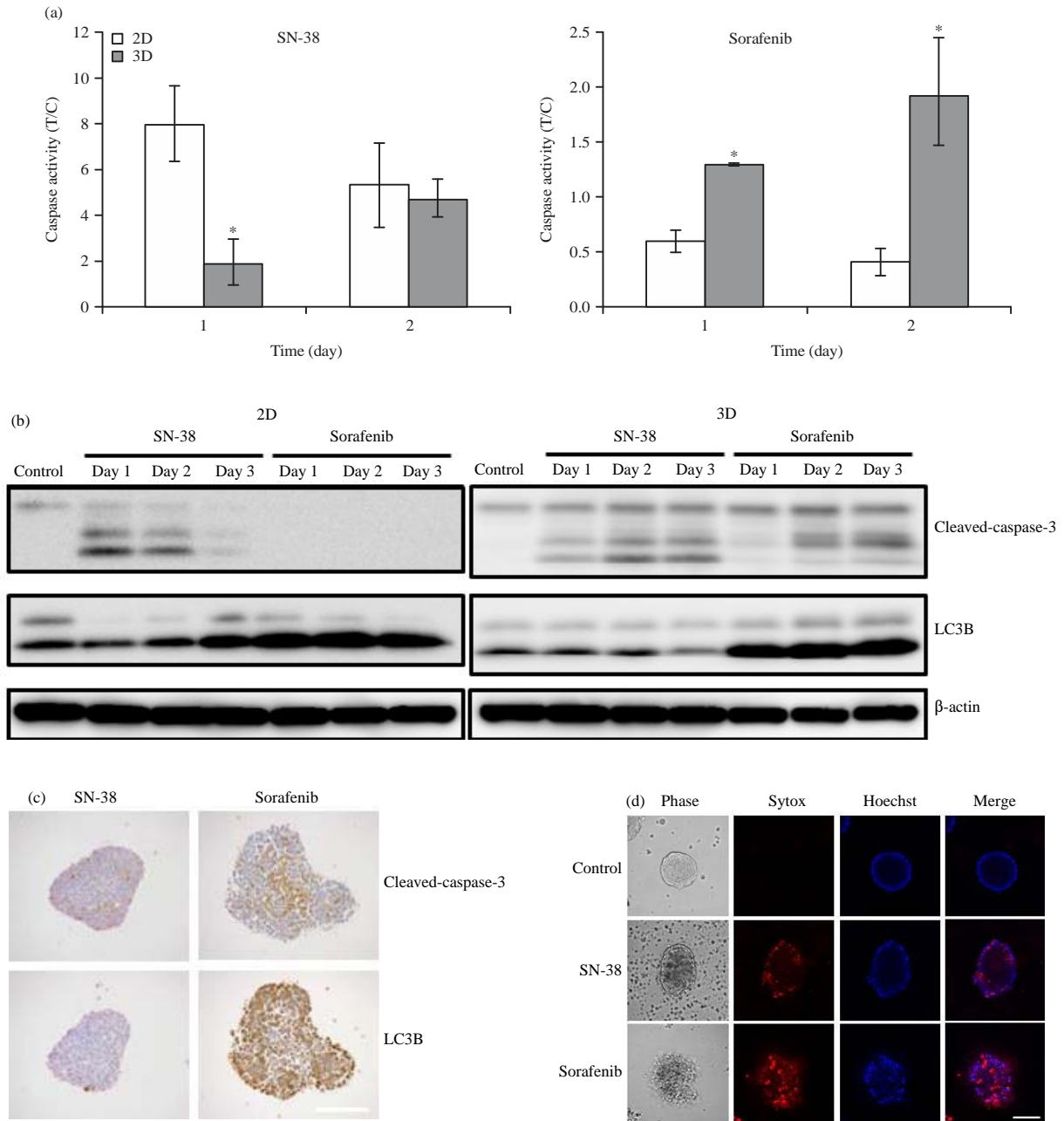


Fig. 3(a-d): Analysis of cell death pathways induced by SN-38 and Sorafenib in 2D and 3D culture condition (a) Caspase-3/7 induction by SN-38 and sorafenib in 2D and 3D culture condition, (b) Cleaved caspase-3, LC3B and b-actin protein expression after 24-72 h compounds exposure by Western blot (c) Immunohistochemistry of compounds treated HCT116 spheroids with antibodies to cleaved caspase-3 and LC3B. Scale bar indicated 100 μ m and (d) Fluorescence micrographs of double staining to Hoechst (blue, index of nuclear) and SYTOX orange (red, index of dead cells) were taken after 48 h compounds exposure. Scale bar indicated 100 μ m

*p<0.05 compared with 2D culture group. Each bar represents the Mean \pm SD

the magnitudes of the death depend on the circumstances among spheroids. In addition, sorafenib induced apoptosis only in the environment formed in the central area of the

spheroids, while non-apoptotic cell death was induced in the peripheral area. To identify the factors that regulate the cell death induction within the spheroid, caspase induction

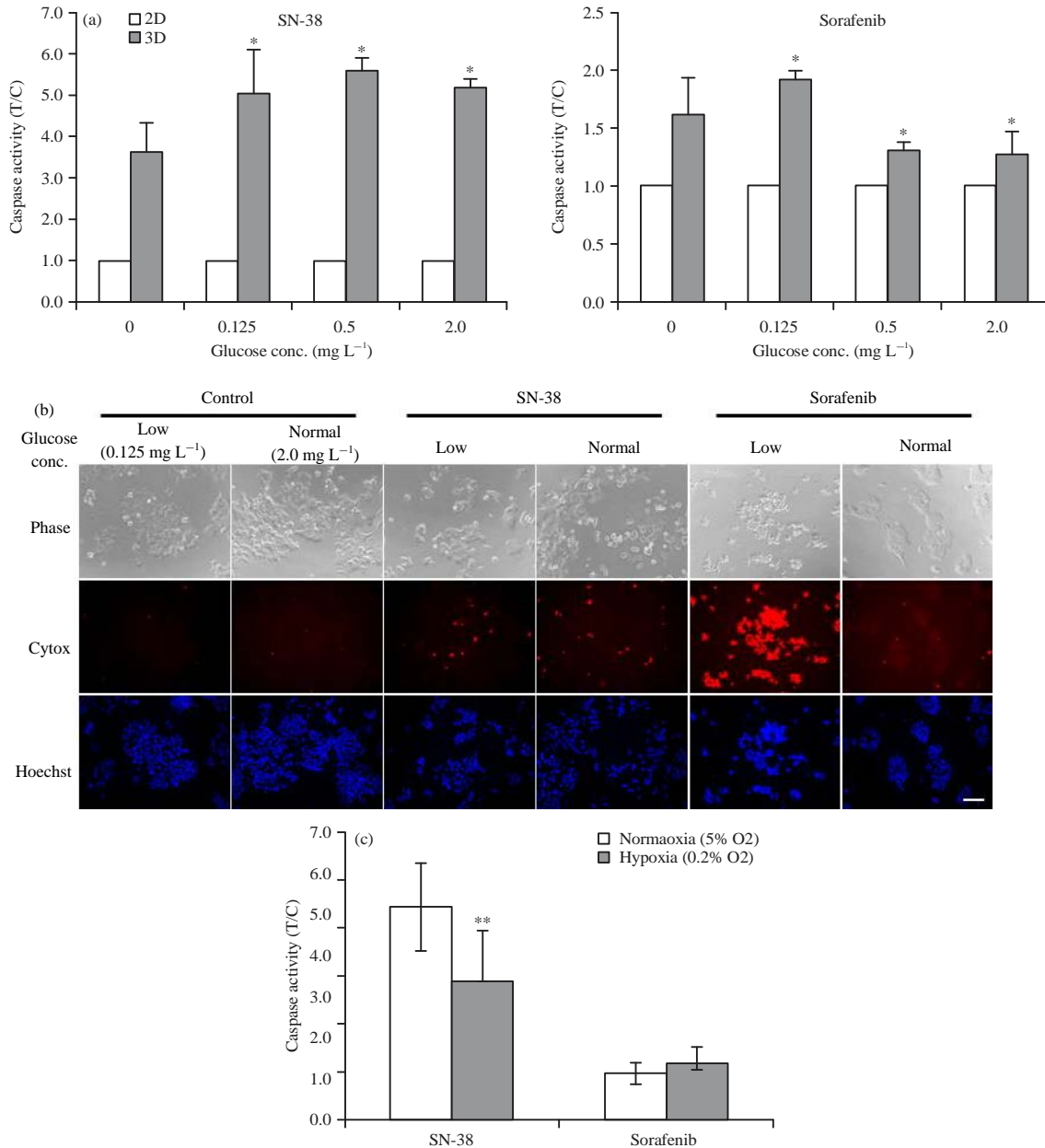


Fig.4(a-c): Effects of culture conditions on apoptosis induction activity of SN-38 and sorafenib (a) Caspase-3/7 induction by SN-38 and sorafenib in various glucose concentrations. HCT116 cells cultured in various glucose conditions are exposed to compounds for 24 h and caspase-3/7 activity was determined using caspase-3/7-Glo, (b) Microscope Images of HCT116 exposed to SN-38 and sorafenib for 24 h in various glucose concentrations. Scale bar indicated 100 μ m and (c) Caspase-3/7 induction by SN-38 and sorafenib hypoxia conditions. HCT116 cells cultured in normoxia or hypoxia conditions are exposed to compounds for 24 h and caspase-3/7 activity was determined using caspase-3/7-Glo. Experiment was conducted three times, each sample was assessed in duplicate. * $p < 0.05$, compared with 2D culture group. ** $p < 0.05$, compared with normoxia group. Each bar represents the Mean \pm SD

activity of compounds were evaluated under the selected circumstances possibly occurring, i.e., low glucose concentration or hypoxia.

First, caspase activities in the different concentrations of glucose (0-2.0 mg L⁻¹) were assessed. Although SN-38 induced

caspase activation in glucose concentration 0.125-2.0 mg L⁻¹, caspase activity was diminished in glucose concentration 0 mg L⁻¹. On the other hand, as shown in Fig. 4a, sorafenib-induced caspase activity was modest at the normal glucose concentration (2.0 mg L⁻¹). Nevertheless, sorafenib enhanced

caspace activity in lower glucose concentrations (0-0.125 mg L⁻¹). These results suggest that low glucose convert the effects of sorafenib to induce caspace activation. For further evaluation of the effects of glucose concentrations on sorafenib mediated cell death, dead cells were identified by SYTOX reagent (Fig. 4b). As expected, SYTOX positive dead cells were markedly detected in sorafenib treated cells at lower glucose concentration (0.125 mg L⁻¹).

Next, caspace activities under reduced oxygen condition were evaluated (Fig. 4c). SN-38 mediated caspace induction was diminished at hypoxic condition. However, sorafenib mediated caspace activation was not altered at hypoxic culture. Taken together, either low glucose concentration or reduced oxygen condition, the extracellular circumstances which appear to occur frequently within the central portion of the spheroids, induce resistance to SN-38 mediated cell death but not sorafenib associated cell death.

DISCUSSION

The results of this study relate to the cell death mechanisms induced by either cytotoxic chemotherapeutic agents or so called molecular targeted agents including tyrosine kinase-inhibitors. The comparison of the cell death sensitivity to those agents between 2D and 3D culture conditions were focused in this study. The results demonstrated that i) cancer cells cultured on the NCP plates formed 3D spheroids, ii) the 3D spheroids were relatively resistant to the cytotoxic chemotherapeutic agents as compared to the cells under 2D culture, iii) the tyrosine kinase inhibitors or the multi-kinase inhibitors diminished cancer cell proliferation under 2D culture as well as under 3D culture condition, iv) SN-38 mediated caspace-3 activation was diminished in cells located in the central area of the 3D spheroids, v) sorafenib induced LC3 cleavage in both 2D and 3D conditions, vi) while sorafenib induced caspace-3 activation only in 3D cultured cells, vii) either glucose reduction or hypoxia suppressed SN-38 associated caspace activation.

The 3D culture system was expected to mimic the phenotypes well in correspondence with *in vivo* or clinical tumors^{5,6}. Tumor cell heterogeneity observed in clinic partly depend on the genetic heterogeneity of tumor cells, while the tumor microenvironments also regulate the heterogeneous phenotypes of the cells²⁰. For example, cancer cells locating apart from the blood vessels are exposed to the nutrient starvation, hypoxia and accumulation of acidic metabolites, because the disorganized vasculature at the tumor site is not able to supply sufficient nutrients and oxygen to cells in this

area²¹. As a consequence, cells in this microenvironment show slow proliferation, low sensitivity to cancer therapies and dependency on mitochondria for energy supply and survival^{22,23}.

In this study, the commercially available NanoCulture plate was used for the 3D culture. This is a reliable technology to culture the cells forming the 3D spheroids from cell lines²⁴. In addition, some studies report the similarity between the spheroids in NCP and *in vivo* or clinical tumors²⁵. For example, human hepatoma cell line HepG2 cultured in NCP showed hepatocyte specific function which was not observed in cells cultured in 2D condition²⁶. It was also reported that human colon cancer cell line HCT116 cultured in NCP showed resistance to conventional cytotoxic compounds i.e., Melphalan, Irinotecan, Oxaliplatin, 5-FU²⁸. Moreover, HCT116 spheroids in NCP has been reported to show the following features, i) heterogeneous localization of Ki-67-positive cells²⁷, ii) up-regulation of genes regarding cell adhesion such as CLDN3, CLDN4 and CDH1²⁷, iii) down-regulation of genes regarding cell cycle and DNA replication, i.e., CDK2, CDK4, cdc25 and, PCNA²⁷, iv) hypoxic area of the center of the spheroids^{25,27}. In the present study, the biological features of the HCT116 spheroids were evaluated and it was confirmed that the 3D culture condition using the NCP was identical to the reported 3D culture system. Immunohistochemistry of Ki-67 showed heterogeneous staining images such as cells located on outer layer of spheroids were strongly stained by Ki-67 compared to cells located in the center. Gene expression analysis of spheroids showed the down-regulation of genes regarding cell cycle and DNA replication represented by CCND1, CDK4 and CDK6. These results indicate that proliferation of cells locating in the center are regulated at gene expression level. In gene expression analysis, up-regulation of tight junction marker CLDN4 and CLDN7 were detected. In addition, up-regulation of CA9 that is the one of the most reliable hypoxic marker regulated by HIF-1a was also detected. These facts indicate that some cells, probably locating in the center of spheroids were under hypoxic condition and separated from external environment.

In 2015, Nomenclature Committee on Cell Death (NCCD) proposed to use the new cell death classification based on quantifiable biochemical parameters²⁸. In this classification, cell death is categorized into two broad, mutually exclusive categories: accidental cell death (ACD) and regulated cell death (RCD). ACD was defined as cell death caused by severe insults, like physical, chemical and mechanical stimuli and insensitive to pharmacologic or genetic interventions of any kind. On the other hands, RCD is defined as cell death involves a genetically encoded molecular machinery and some RCD

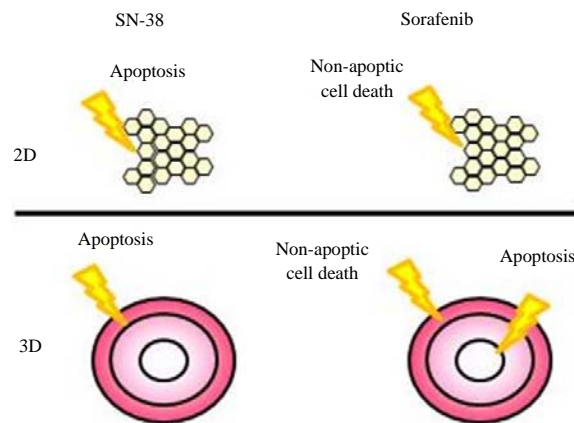


Fig. 5: Proposed cell death induction model of SN-38 and sorafenib in 2D and 3D culture conditions

occurs in the context of post-embryonic development, tissue homeostasis and immune responses are categorized as programmed cell death (PCD). Regarding cell death characterization, many reports have suggested that most of cytotoxic agents used for conventional chemotherapies show their anti-proliferation effects by inducing caspase-dependent cell death or apoptosis²⁹⁻³³. SN-38 was a representative cytotoxic agent and known to induce caspase-dependent apoptotic death³⁴. It was also reported that SN-38 cytotoxicity is cell cycle-dependent³⁵. On the other hands, not only apoptosis but also other PCD are reported as cell death activated in cells treated by kinase inhibitors³⁶. In the present study, the results from 2D cultured cells showed that apoptotic death was induced by cytotoxic drugs, while non-apoptotic RCD was mediated by kinase inhibitors. Recent studies suggest that not only apoptosis but also other RCD concomitant with LC3B are induced in the cells treated by kinase inhibitors³⁶⁻⁴⁰. These reports are consistent with the results that sorafenib induced cell death concomitant with LC3B expression in 2D culture condition.

Results from the 3D cultured cells suggested that SN-38 induced apoptosis was limited only in cells located on the surface area of the spheroids. As reported before, cells in the center of spheroids show slow proliferation, low sensitivity to cancer drugs and are under hypoxia condition²⁷. Additionally, cells in hypoxia may show resistance to apoptotic cell death^{40,41}. In clinical tumors, these phenotypes are seen in cells apart from blood vessel²¹ and these cells also are exposed to the nutrient starvation resulting in the dependency on mitochondria for energy supply and survival^{6,21,23,24,40}. These results may consistent with the scenario showing the possibility that cancer cells in the central area may obtain apoptosis resistance in 3D spheroids (Fig. 5).

It is worth noting that sorafenib induced significant apoptosis in the central area of the 3D spheroids. In addition, significant caspase activation and cell death were also identified in glucose reduced 2D culture condition. These results raise the possibility that glucose concentration may regulate the conversion of types of sorafenib mediated cell death. In normal glucose condition, cancer cells use aerobic glycolysis for energy production (known as Warburg effect). However, in low glucose condition, cells are not able to supply their energy requirement by glycolysis. In other words, cells in low glucose condition cannot but depend on mitochondria for their energy requirement. This fact was supported by the results that many mitochondria inhibitors have been identified as a result of screening conducted under conditions of nutrient starvation²². Thus, drugs affecting mitochondrial energy production may modulate the cell death pathway including mitochondria associated cell death pathway. Indeed, it was reported that sorafenib has direct inhibitory effects on mitochondrial function^{18,19}. These facts indicate that, in low glucose condition, sorafenib critically effects on energy production. In conjunction with these reports, these results suggest that sorafenib effects on energy production by inhibiting mitochondrial function and induces apoptosis to the cells under low glucose condition like center on spheroids.

CONCLUSION

In conclusion, cancer cells cultured under 3D condition are resistant to cytotoxic chemotherapeutic agents. Multi-kinase inhibitors including sorafenib induces significant apoptosis in cells located in the central area of the 3D cultured spheroids, resulting in effective cytotoxicity against the cells, whose sensitivity to conventional chemotherapeutic drugs is

limited. The conversion of the mechanisms of sorafenib associated cell death, i.e., non-apoptotic cell death or apoptotic cells, appears to be regulated by the extracellular condition including glucose concentration. These results provided a new insight into the mechanisms of kinase-inhibitor mediated cell death in the 3D cultured cancer cells. The heterogeneous extracellular condition may also occur within *in vivo* tumors, therefore, the 3D culture condition used in the present study would appear to be useful for a handy drug sensitivity testing partially mimicking *in vivo* condition.

SIGNIFICANCE STATEMENTS

This study discovers the differences of the action of anti-cancer drugs in the 2D- and 3D-culture conditions. This study help the researcher to uncover the critical area of innovative anti-cancer drug discovery that many researchers were not able to explore. The 3D cell culture system can be beneficial for screening the new anticancer drugs.

REFERENCES

1. DiMasi, J.A. and H.G. Grabowski, 2007. Economics of new oncology drug development. *J. Clin. Oncol.*, 25: 209-216.
2. Mazzoleni, G., D. Di Lorenzo and N. Steimberg, 2009. Modelling tissues in 3D: The next future of pharmacotoxicology and food research? *Genes Nutr.*, 4: 13-22.
3. Abbott, A., 2003. Cell culture: Biology's new dimension. *Nature*, 424: 870-872.
4. Bissell, M.J. and D. Radisky, 2001. Putting tumours in context. *Nat. Rev. Cancer*, 1: 46-54.
5. Breslin, S. and L. O'Driscoll, 2013. Three-dimensional cell culture: The missing link in drug discovery. *Drug Discov. Today*, 18: 240-249.
6. Hirschhaeuser, F., H. Menne, C. Dittfeld, J. West, W. Mueller-Klieser and L.A. Kunz-Schughart, 2010. Multicellular tumor spheroids: An underestimated tool is catching up again. *J. Biotechnol.*, 148: 3-15.
7. Strumberg, D., H. Richly, R.A. Hilger, N. Schleucher and S. Korfee *et al.*, 2005. Phase I clinical and pharmacokinetic study of the novel Raf kinase and vascular endothelial growth factor receptor inhibitor BAY 43-9006 in patients with advanced refractory solid tumors. *J. Clin. Oncol.*, 23: 965-972.
8. Escudier, B., T. Eisen, W.M. Stadler, C. Szczylik and S. Oudard *et al.*, 2007. Sorafenib in advanced clear-cell renal-cell carcinoma. *N. Engl. J. Med.*, 356: 125-134.
9. Gupta-Abramson, V., A.B. Troxel, A. Nellore, K. Puttaswamy and M. Redlinger *et al.*, 2008. Phase II trial of sorafenib in advanced thyroid cancer. *J. Clin. Oncol.*, 26: 4714-4719.
10. McCormack, P.L., 2014. Pazopanib: A review of its use in the management of advanced renal cell carcinoma. *Drugs*, 74: 1111-1125.
11. Sternberg, C.N., R.E. Hawkins, J. Wagstaff, P. Salman and J. Mardiak *et al.*, 2013. A randomised, double-blind phase III study of pazopanib in patients with advanced and/or metastatic renal cell carcinoma: Final overall survival results and safety update. *Eur. J. Cancer*, 49: 1287-1296.
12. Grothey, A., E. van Cutsem, A. Sobrero, S. Siena and A. Falcone *et al.*, 2013. Regorafenib monotherapy for previously treated metastatic colorectal cancer (CORRECT): An international, multicentre, randomised, placebo-controlled, phase 3 trial. *Lancet*, 381: 303-312.
13. Li, J., S. Qin, R. Xu, T.C. Yau and B. Ma *et al.*, 2015. Regorafenib plus best supportive care versus placebo plus best supportive care in Asian patients with previously treated metastatic colorectal cancer (CONCUR): A randomised, double-blind, placebo-controlled, phase 3 trial. *Lancet Oncol.*, 16: 619-629.
14. Fan, L.C., H.W. Teng, C.W. Shiau, W.T. Tai and M.H. Hung *et al.*, 2016. Regorafenib (Stivarga) pharmacologically targets epithelial-mesenchymal transition in colorectal cancer. *Oncotarget*, 7: 64136-64147.
15. Llovet, J.M., S. Ricci, V. Mazzaferro, P. Hilgard and E. Gane *et al.*, 2008. Sorafenib in advanced hepatocellular carcinoma. *N. Engl. J. Med.*, 359: 378-390.
16. Montella, L., G. Palmieri, R. Addeo and S. Del Prete, 2016. Hepatocellular carcinoma: Will novel targeted drugs really impact the next future? *World J. Gastroenterol.*, 22: 6114-6126.
17. Dent, P., 2013. Multi-kinase modulation for colon cancer therapy. *Cancer Biol. Ther.*, 14: 877-878.
18. Bull, V.H., K. Rajalingam and B. Thiede, 2012. Sorafenib-induced mitochondrial complex I inactivation and cell death in human neuroblastoma cells. *J. Proteome Res.*, 11: 1609-1620.
19. Will, Y., J.A. Dykens, S. Nadanaciva, B. Hirakawa and J. Jamieson *et al.*, 2008. Effect of the multitargeted tyrosine kinase inhibitors imatinib, dasatinib, sunitinib and sorafenib on mitochondrial function in isolated rat heart mitochondria and H9c2 cells. *Toxicol. Sci.*, 106: 153-161.
20. Gillies, R.J. and R.A. Gatenby, 2015. Metabolism and its sequelae in cancer evolution and therapy. *Cancer J.*, 21: 88-96.
21. Horsman, M.R. and P. Vaupel, 2016. Pathophysiological basis for the formation of the tumor microenvironment. *Front. Oncol.*, Vol. 6. 10.3389/fonc.2016.00066.
22. Zhang, X., A. de Milito, M.H. Olofsson, J. Gullbo, P. D'Arcy and S. Linder, 2015. Targeting mitochondrial function to treat quiescent tumor cells in solid tumors. *Int. J. Mol. Sci.*, 16: 27313-27326.
23. Brown, J.M. and W.R. Wilson, 2004. Exploiting tumour hypoxia in cancer treatment. *Nat. Rev. Cancer.*, 4: 437-447.

24. Rimann, M. and U. Graf-Hausner, 2012. Synthetic 3D multicellular systems for drug development. *Curr. Opin. Biotechnol.*, 23: 803-809.
25. Yoshii, Y., A. Waki, K. Yoshida, A. Kakezuka and M. Kobayashi *et al.*, 2011. The use of nanoimprinted scaffolds as 3D culture models to facilitate spontaneous tumor cell migration and well-regulated spheroid formation. *Biomaterials*, 32: 6052-6058.
26. Nakamura, K., N. Kato, K. Aizawa, R. Mizutani, J. Yamauchi and A. Tanoue, 2011. Expression of albumin and cytochrome P450 enzymes in HepG2 cells cultured with a nanotechnology-based culture plate with microfabricated scaffold. *J. Toxicol. Sci.*, 36: 625-633.
27. Fujiwara, D., K. Kato, S. Nohara, Y. Iwanuma and Y. Kajiyama, 2013. The usefulness of three-dimensional cell culture in induction of cancer stem cells from esophageal squamous cell carcinoma cell lines. *Biochem. Biophys. Res. Commun.*, 434: 773-778.
28. Galluzzi, L., J.M. Bravo-San Pedro, I. Vitale, S.A. Aaronson and J.M. Abrams *et al.*, 2015. Essential *versus* accessory aspects of cell death: Recommendations of the NCCD 2015. *Cell Death Differ.*, 22: 58-73.
29. Katsman, A., K. Umezawa and B. Bonavida, 2007. Reversal of resistance to cytotoxic cancer therapies: DHMEQ as a chemo-sensitizing and immuno-sensitizing agent. *Drug Resistance Updates*, 10: 1-12.
30. Bates, D.J. and L.D. Lewis, 2013. Manipulating the apoptotic pathway: Potential therapeutics for cancer patients. *Br. J. Clin. Pharmacol.*, 76: 381-395.
31. Hajj, C., K.A. Becker-Flegler and A. Haimovitz-Friedman, 2015. Novel mechanisms of action of classical chemotherapeutic agents on sphingolipid pathways. *Biol. Chem.*, 396: 669-679.
32. Weekes, J., A.K. Lam, S. Sebesan and Y.H. Ho, 2009. Irinotecan therapy and molecular targets in colorectal cancer: A systemic review. *World J. Gastroenterol.*, 15: 3597-3602.
33. Hector, S. and J.H.M. Prehn, 2009. Apoptosis signaling proteins as prognostic biomarkers in colorectal cancer: A review. *Biochim. Biophys. Acta (BBA)-Rev. Cancer*, 1795: 117-129.
34. Lansiaux, A., R.A. Bras-Goncalves, C. Rosty, P. Laurent-Puig, M.F. Poupon and C. Bailly, 2001. Topoisomerase I-DNA covalent complexes in human colorectal cancer xenografts with different p53 and microsatellite instability status: relation with their sensitivity to CTP-11. *Anticancer Res.*, 21: 471-476.
35. Fujita, K.I., Y. Kubota, H. Ishida and Y. Sasaki, 2015. Irinotecan, a key chemotherapeutic drug for metastatic colorectal cancer. *World J. Gastroenterol.*, 21: 12234-12248.
36. Rikiishi, H., 2012. Autophagic action of new targeting agents in head and neck oncology. *Cancer Biol. Ther.*, 13: 978-991.
37. Heqing, Y., L. Bin, Y. Xuemei and L. Linfa, 2016. The role and mechanism of autophagy in sorafenib targeted cancer therapy. *Crit. Rev. Oncol./Hematol.*, 100: 137-140.
38. Panka, D.J., W. Wang, M.B. Atkins and J.W. Mier, 2006. The Raf inhibitor BAY 43-9006 (Sorafenib) induces caspase-independent apoptosis in melanoma cells. *Cancer Res.*, 66: 1611-1619.
39. Panka, D.J., D.C. Cho, M.B. Atkins and J.W. Mier, 2008. GSK-3 β inhibition enhances sorafenib-induced apoptosis in melanoma cell lines. *J. Biol. Chem.*, 283: 726-732.
40. Wilson, W.R. and M.P. Hay, 2011. Targeting hypoxia in cancer therapy. *Nat. Rev. Cancer*, 11: 393-410.
41. Wigerup, C., S. Pahlman and D. Bexell, 2016. Therapeutic targeting of hypoxia and hypoxia-inducible factors in cancer. *Pharmacol. Therapeut.*, 164: 152-169.